Annals of Biomedical Engineering, Vol. 24, pp. 99–108, 1996
Printed in the USA.

0090-6964/96 $10.50 + .00

Membrane Potential Fluctuations of Human T-Lymphocytes Have Fractal Characteristics of Fractional Brownian Motion

ALBERT M. CHURILLA,* WOLFRAM A. GOTTSCHALKE,* LARRY S. LIEBOVITCH,†
LEV Y. SELECTOR,‡ ANGELO T. TODOROV,† and STEPHEN YEANDLE*

*Naval Medical Research Institute, Bethesda, MD; †Florida Atlantic University, Center for Complex Systems, Boca Raton, FL; and ‡Columbia University, Department of Ophthalmology, New York, NY

Abstract—The voltage across the cell membrane of human T-lymphocyte cell lines was recorded by the whole cell patch clamp technique. We studied how this voltage fluctuated in time and found that these fluctuations have fractal characteristics. We used the Hurst rescaled range analysis and the power spectrum of the increments of the voltage (sampled at 0.01-sec intervals) to characterize the time correlations in these voltage fluctuations. Although there was great variability in the shape of these fluctuations from different cells, they all could be represented by the same fractal form. This form displayed two different regimes. At short lags, the Hurst exponent $H = 0.76 \pm 0.05$ (SD) and, at long lags, $H = 0.26 \pm 0.04$ (SD). This finding indicated that, over short time intervals, the correlations were persistent ($H > 0.5$), that is, increases in the membrane voltage were more likely to be followed by additional increases. However, over long time intervals, the correlations were antipersistent ($H < 0.5$), that is, increases in the membrane voltage were more likely to be followed by voltage decreases. Within each time regime, the increments in the fluctuations had characteristics that were consistent with those of fractional Gaussian noise (fGn), and the membrane voltage as a function of time had characteristics that were consistent with those of fractional Brownian motion (fBm).

Keywords—Long-term correlations, Hurst rescaled range analysis, Power spectrum, Nonlinear, Intracellular PD.

INTRODUCTION

The membrane potential is the electrical potential inside the cell minus the electrical potential in the solution outside the cell. This potential is an important indicator of the state of a cell. To measure the changes in membrane potential that occur when T-lymphocytes are activated or otherwise changed, we first must characterize the properties of the resting membrane potential.

The membrane potential of T-lymphocytes has been measured with intracellular glass micropipette electrodes and voltage-sensitive dyes. These methods yielded values of -5 mV to -70 mV for the resting membrane potential (10,11,24). These studies reported the average value of the membrane potential measured in each cell, but they were not concerned with how the potential varied with time. Other studies in which the whole cell configuration of the patch clamp technique was used did evaluate some of the properties of the temporal fluctuations in the potential (20,21). However, these studies did not provide information about the quantitative properties of these fluctuations or suggest a stochastic process that could characterize them. We report here the results of our analysis of membrane potential fluctuations from whole cell patch recordings of T-lymphocytes from various clones.

The motivation for our analysis can be seen in Fig. 1. Graph B shows the values of a time series of a process called fractional Gaussian noise (fGn) (8,22). Graph A illustrates a running sum of the values of the graph B and is called fractional Brownian motion (fBm) (8,22). This fBm has fractal characteristics; as the record is examined over ever-larger time intervals, there are ever-larger fluctuations in amplitude. This fractal property is called statistical self-similarity. Formally, this means that the average value of a property, such as the amplitude, is directly proportional to the size of the time window used to make the measurement (3,16). Graph C in Fig. 1 shows the values of the membrane potential recorded from a T-lymphocyte, and graph D shows the time series of the differences of the consecutive values of the

Acknowledgment—We thank Ruth Ann Donnelly for technical support during the early stages of this investigation and Dr. Karoli Meszaros for many helpful discussions and technical support. Supported in part by the Naval Medical Research and Development Command, Research Task M2022.001-1110.

The opinions and assertions contained herein are the private ones of the authors and are not to be construed as official or reflecting the views of the Navy Department or the naval service at large.

This work was also supported in part by National Institutes of Health Grant EY-6234 and was done under the tenure of an Established Investigatorship from the American Heart Association awarded to L. S. Liebovitch.

Address correspondence to Dr. L. S. Liebovitch, Florida Atlantic University, Center for Complex Systems, 777 Glades Road, Boca Raton, FL 33431, U.S.A.

(Received 15May95, Revised 30June95, Revised, Accepted 11Aug95)

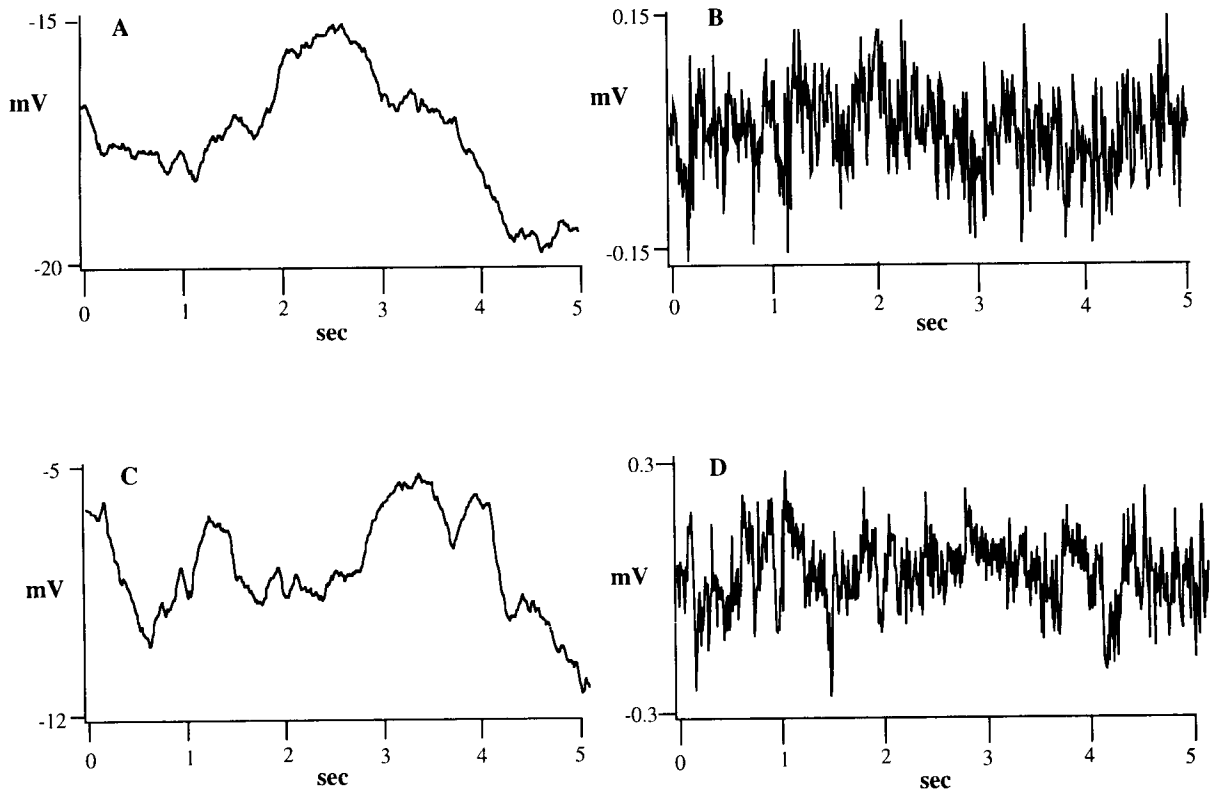

FIGURE 1. (Top): A shows the time series of the fractal process fBm, which is constructed from the running sum of the time series fGn, shown in B. (Bottom): Typical membrane potential recorded from a T-lymphocyte with use of the whole cell patch clamp technique. C shows the membrane potential as a function of time. D shows the differences between successive values of the membrane potential recorded every 0.01 sec. The similarity in form between the fractal simulations shown in the top graphs and the membrane potential shown in the bottom graphs suggested to us that it would be worthwhile to investigate in more detail whether the fluctuations in the membrane potential had fractal properties.

membrane potential sampled every 0.01 sec. The apparent similarity between the numerical simulation of the fractal process in graphs A and B in Fig. 1 and the measurement of the membrane potential in graphs C and D in Fig. 1 suggested to us that the stochastic processes of fGn and its integral, fBm, might be a way to characterize the voltage increments and the voltage, respectively, across the membrane of T-lymphocytes. To test this hypothesis, we used two fractal methods of analysis: Hurst rescaled range analysis and power spectrum. Fractals have statistical properties that are different from those of nonfractals (2). Because the experimental data appear to have a fractal form, a fractal analysis may provide more valid quantitative measures of the time correlations in the membrane potential than those given by nonfractal methods of analysis.

In the last 25 years, nonlinear systems with fractal properties have generated interest in many fields of science. New concepts and techniques developed to study objects and processes with fractal properties have yielded new insight into how such systems work. The mathematical properties of fractals and their applications to physical systems are described in References 8 and 22. Elementary introductions to fractals and their application to biological systems are given in References 3, 14, 15, and 16. First, we review in brief some of the most important properties of the fractals and their relevance to the work presented here.

An essential characteristic of fractals is that if the resolution is increased, ever-smaller features are revealed, that is, more and more new pieces are seen. These pieces are self-similar, which means that the statistical distribution of the pieces at one resolution has the same shape as does the distribution of the pieces at other resolutions (2). The mathematical properties of fractals are defined through the use of measure theory and topology. Formally, a fractal is defined as an object or process that has a fractal dimension (which characterizes how the number of resolved pieces of an object depend on the resolution) that is greater than the topological dimension (an integer dimension that depends on how the pieces are connected together). This technical definition and its implications are explained in detail in Reference 2.

The moments of fractal processes, such as the mean and variance, depend on the number of pieces included at a given resolution. Because the number of these pieces depends on the resolution, the moments do not have fixed,

limiting values. The values determined for the moments, therefore, depend on the resolution used to make the measurement. For example, when the fluctuations of a time series are fractal, then the differences between the maximum and minimum values of the time series increase with time. Therefore, the range of the time series increases with the length of the piece of the series examined. Therefore, as more data are analyzed, the value of the standard deviation will increase continually and will never reach a finite limiting value. Nonfractal methods, such as those that assume that the data can be represented by processes that are Gaussian or asymptotically Gaussian, assume that these moments exist and have finite values. Therefore, such nonfractal methods cannot properly characterize the type or degree of correlations present in fractal data. We must use appropriate fractal methods to be able to successfully characterize the correlations present in a fractal time series. Properly characterizing these fractal properties may lead us to a better understanding of the processes that produced the data.

The fractal form of the voltage fluctuations suggests that, to characterize the type and degree of correlations in the experimental data, we should determine how the value of the dispersion depends on the size of the window used to evaluate it. This can be done in a number of ways. We did this by using the Hurst rescaled range analysis and the power spectrum analysis.

METHODS

Cells

Experiments were performed on Jurkat cells, a human leukemic T cell line; CL1 cells, a $CD4^+/CD8^-$ anti-*Rickettsia tsutsugamushi* cell line, and Ka8, a $CD4^+/CD8^-$ population cloned from CL1. The Jurkat cells were maintained in culture RPMI medium (GIBCO-BRL, Grand Island, NY) supplemented with penicillin, streptomycin, glutamine, 5×10^{-4} M 2-mercaptoethanol and 5% (v/v) fetal calf serum (FCS). CL1 was obtained from spleen cells of C3H/HeJ mice immunized with live *R. tsutsugamushi* bacteria. Ka8 was cloned by a limiting dilution in the presence of antigen (French Press lysates of *R. tsutsugamushi* in RPMI medium supplemented with penicillin, streptomycin, glutamine, 2-mercaptoethanol, and 10% FCS. Both CL1 and Ka8 cells were maintained by passage every 7–10 days in the presence of antigen (French Press lysates of *R. tsutsugamushi*) and irradiated spleen cells.

Experiments

All data were obtained by the patch-clamp technique in the whole cell configuration (5,29). Micropipettes were pulled in multiple stages by a Flaming/Brown Model P-87 pipette puller (Sutter Instruments, San Rafael, CA) and fire polished. They were made from Accu-fill 90 Micropet glass obtained from Clay Adams (Parsippany, NJ) and filled through an Acrodisc 13, 0.2 μ filter (Gelman Sciences, Ann Arbor, MI) with the following solution (in mM): 140 KCl, 0.1 $CaCl_2$, 1.0 $MgCl_2$, and 10 HEPES buffer at pH = 7.3 and 1.1 EGTA. The experiments were performed at room temperature (20–22°C). Chemicals were purchased from the Sigma Chemical Co. (St. Louis, MO). Pipette resistances typically were 1–4 MΩ. Total junction potential was no more than 1–2 mV.

In all experiments, the cells were placed in a solution containing the following (in mM): 145 NaCl, 4.5 KCl, 1.6 $CaCl_2$, 1.1 $MgCl_2$, and 10 HEPES buffer, pH = 7.3. Additional details of the experiments were described in Reference 31. In the whole cell configuration, the solution in the patch pipette replaced the solution inside the cell. Therefore, some factors controlling the membrane potential may be different from those in intact cells. We waited 3–10 min after achieving the whole cell configuration before taking measurements.

Membrane potential as a function of time was measured with an EPC-7 patch clamp amplifier in the zero constant current mode, and the data were stored on a VCR using a Neuro-corder Model DR-384 pulse code modulator (Neuro Data Instruments, New York, NY). A 5-kHz, 8-pole, low-pass, Bessel filter was connected to the input of the Neuro-corder.

Voltage clamp data were collected with the Axon Instruments (Foster City, CA) software package pCLAMP 5.5, running on an PC-AT computer containing a Labmaster board. Results were stored on the computer's hard disk. For each cell, a sequence of depolarizing pulses (190 ms long, 5 sec apart) was applied from a holding potential of −70 mV. There were 13 pulses in the sequence (from −60 mV to +60 mV); each step was 10 mV more positive than the preceding step.

The parallel combination of cell resistance and seal resistance, which we called the whole cell membrane resistance, was estimated from the difference between the current at a holding potential of −70 mV, just before the first pulse of the above-described voltage clamp protocol, and the current, immediately before the end of this pulse, when the voltage was −60 mV. This jump in membrane potential was too small to produce an appreciable active current (5). The pipette and cell capacitances were partially compensated. By the end of the pulse, the capacitive currents were too small to be detected.

Data Processing

To analyze the membrane potential, the data were played back from the Neuro-corder through a 60 Hz low

pass, 8-pole Bessel filter to the 12-bit A/D converter of the Labmaster board in the PC-AT computer. The computer was running the Axon Instruments Software package, Axotape 1.2 (Axon Instruments). The records were stored on a hard disk. The digitizing rate was 100 points/sec. The resulting files were analyzed by using Asyst 4.0 software (Keithley Asyst, Taunton, MA) on an IBM PC-AT computer, and by using Igor Pro 2.01 software (Wavemetrics, Lake Oswego, OR) and programs written in QuickBASIC (Microsoft, Bellevue, WA) on an Apple Macintosh IIfx computer.

Rescaled Range Analysis

Our chief method of analysis was the rescaled range analysis developed by Hurst (discussed in 2,8,22). Hurst used it to study time correlations in the annual discharge of the Nile River. He did this to determine the volume that would be needed for the reservoir to be formed by the Aswan High Dam (12). We believe that this is the first use of Hurst's technique to analyze cell membrane potentials. This analysis, in effect, compared the correlations in the time series measured at different time scales. If the data were fractal, then the correlations at different time scales would be shown to be related to each other.

Many descriptions of this method do not make it sufficiently clear whether the input values into the rescaled range method should be the values of the original time series or the differences between successive values. As shown in Fig. 1, we observed that the time series of the voltages recorded across the cell membrane of a human T-lymphocytes seemed to be a random walk of the form of fBm and that the differences between consecutively recorded voltages seemed to have the form of fGn. When this is the case, then the appropriate time series to use in the rescaled range analysis is the increments of the walk, which correspond here to the differences between consecutively recorded voltages. Therefore, we used the differences, $x(i)$,between the successively measured values of the voltage as the input into the Hurst rescaled range analysis, namely, $x(i) = v(i + 1) - v(i)$; where $v(i)$ is the voltage recorded across the cell membrane at time $t_i = idt$, and the time dt between samples of the voltage was 0.01 s.

There is a fractal statistical process that has been described in detail (8,9,19,22). In this process, a time series $z(i)$ is generated by sampling $z(t)$ every dt units of time. The average of the increments $\langle z(i + 1) - z(i)\rangle$ is equal to 0, whereas the variance of the increments $\langle z(i + 1) - z(i))^2$ is proportional to $(dt)^{2H}$, here $t_{i+1} = idt + dt = t_i + dt$ and $t_i = idt$. The time series of the increments $z(i + 1) - z(i)$ is fGn and the time series of $z(i)$ is fBm. In our case, $z(i)$ corresponded to the membrane voltage $v(i)$ and the increments $z(i + 1) - z(i)$ corresponded to the differences between the successively measured values of the voltage $x(i)$.

To test the accuracy of our methods we analyzed test time series of fGn that we generated with known values of H. The test time series were generated by using the method described by Feder (8) and implemented in a BASIC program published by Peters (26). (For those interested in using this method, please note that there is a typographical error in Eq. 9.25, which defines this method, in the third printing of Feder's book, which was corrected in the fourth printing, and that there are also two obvious typographical errors in the BASIC program in Peter's book.) The values of H that we determined from the rescaled range analysis closely reflected the values of H used to generate the test time series. However, we also found, as reported previously by Schepers *et al.* (30) and Bassingthwaighte and Raymond (3), that there small (0% to 15%) systematic errors exist between the values of H determined from the rescaled range analysis and the values of H used to generate the fGn. The use of such test data with known properties helped us to verify the accuracy of our programs and confirmed that the appropriate time series to use in the analysis was the increments, namely, fGn, rather than the time series of the fBm itself.

The time series used in the rescaled Hurst analysis, $x(i)$ was the differences of the consecutive values from the membrane potential. Each time series contained $2^{13} = 8{,}192$ points and was divided into adjacent segments, each of M points. M always was an integral power of two and ranged between 2 and 8,192. The time between successive points in the time series was 0.01 sec for all experiments. $N(M)$, the number of segments of length M, was $8192/M$ and was an integer, because both 8,192 and M were powers of 2. To perform the rescaled range analysis requires that we compute a quantity called R/S for each M.

The mean, $\langle x\rangle_{n,M}$, of the n-th segment of length M was

$$\langle X\rangle_{n,M} = \frac{1}{M}\sum_{i=(n-1)M+1}^{nM} x(i)$$

The standard deviation $S_{n,M}$ of the n-th segment of length M was

$$S_{n,M} = \left[\left(\frac{1}{M}\right)\sum_{i=(n-1)M+1}^{nM}(x(i) - \langle x\rangle_{n,M})^2\right]^{1/2}$$

For each point i in the time series we computed

$$Y_{n,M}(i) = \sum_{k=(n-1)M+1}^{i}(x(k) - \langle x\rangle_{n,M})$$

for $(n - 1)M + 1 \leq i \leq nM$. The range $R_{n,M}$ in the n-th segment was then computed by subtracting the least value

of $Y_{n,M}(i)$ from the greatest value of $Y_{n,M}(i)$. We divided the range by the standard deviation to determine the rescaled range. We let

$$(R/S)_{n,M} = (R_{n,M})/(S_{n,M})$$

denote the rescaled range of the *n-th* segment of length M. An average rescaled range, denoted by $(R/S)_M$, was then defined by

$$(R/S)_M = \left(\frac{1}{N(M)}\right) \sum_{n=1}^{N(M)} (R/S)_{n,M}$$

For each time series of 8,192 points, $(R/S)_M$ was calculated for each of the 13 possible values of M.

This algorithm can be thought of as calculating the value of the statistic R/S for time windows of different durations M. Because we sampled the membrane potential every 0.01 sec the lag, T, in sec, is $T = 0.01\ M$. $(R/S)_M$ is called R/S, a function of the lag. The logarithm of R/S was then plotted *versus* the logarithm of T. The slope of this plot was H, the Hurst exponent, the significance of which is discussed below.

It can be shown from the definition of R/S that when $M = 2$ and the two values $x(i)$ are not equal to each other, then R/S is identically equal to 1. When the two values $x(i)$ are equal to each other, then $R = 0$, and $S = 0$ and, hence, R/S is indeterminate. For this latter case, we set $R/S = 1$. (In no cases in our experimental data were four consecutives values of $x(i)$ equal.

Power Spectrum

Time series of 8,192 points of the membrane potential were loaded into Igor Pro 2.01 software (WaveMetrics) on an Apple Macintosh computer. The power spectrum (4,27) of the differences between successive values of the membrane potential sampled at 0.01 sec was then computed by using the standard subroutine for power spectrum density calculation provided with the Igor Pro 2.01 software (WaveMetrics), which took overlapping segments of 2,048 points from the 8,192 points, windowed them, and averaged the squared amplitudes of their FFTs. As is customary, we used a window function to eliminate the effect of the finite number of data points in computing the power spectrum (4,27). For our data, we found that there was no significant difference between the spectrum computed with no window and the Hamming, Hanning, and Blackman-Harris window functions. A least squares fit was used to determine the slope on this logarithmic plot. This slope was subject to an approximately 10% variation as a result of the possible different choices of the range used in the fit.

RESULTS

T-lymphocytes tend to have very high whole cell membrane resistances. Some researchers consider values of 10 GΩ or greater to be normal (5). In our experiments, resistances varied from 0.5–10 GΩ. No single parameter indicated cell viability. Sometimes, cells with low resistance had normal resting potential, and, sometimes, cells with low absolute values of resting potential had normal current responses to voltage pulses. There was no consistent criterion to identify which was a good, natural cell. Typically, the maximum transient ionic current recorded under voltage clamp conditions was about 0.5 nA, although in one of the cells it was 2 nA.

For detailed analysis we picked five cells, designated by the letters A, B, C, D, and E. The membrane potential fluctuations of these cells were representative of the different types of fluctuations observed. Three of the cells, A, B, and E were selected from the murine T cell line CL1. One, C, was from the cloned leukemia line, Jurkat, and one, D, was from the Ka8 clone. Use of the antigen-specific, nontransformed murine T cell line, CL1, and clone, Ka8, allowed us to probe a homogeneous population of "normal" cells, in addition to Jurkat. In these studies, Jurkat was recultured the day before to ensure that all cells were actively proceeding through the cell cycle. Likewise, CL1 and Ka8 were used early after reactivation by specific antigen to ensure maximum cell cycle progression.

The membrane potentials, recorded under zero current clamp, as a function of time for five different cells are shown in Fig. 2. Each of these graphs was a 5-sec, 500-point, representative interval excised from a longer record of 8,192 points. Although the membrane potential fluctuations for different cells differed greatly from one another these fluctuations appear to be self-similar in any given cell. That is, portions of any given record resemble the other portions of the record, with the exception of the spike in Fig. 2E. On visual inspection, these fluctuations appeared to be self-similar in any given cell having a form similar to the fractal form shown in Fig. 1A.

Rescaled Range Analysis

To test quantitatively whether these fluctuations of the membrane were fractal we used the Hurst rescaled range analysis. We plotted logarithm (R/S) *versus* logarithm (T). If R/S was proportional to T^H then the time series had fractal properties.

The plots of logarithm (R/S) *versus* logarithm (T) shown in Fig. 3 have two distinct regimes, each of which could be fitted separately by a straight line. This showed that H, the Hurst exponent, was defined within each regime. A fractal process, such as fGn, will produce a straight line on such a plot. Therefore, the existence of

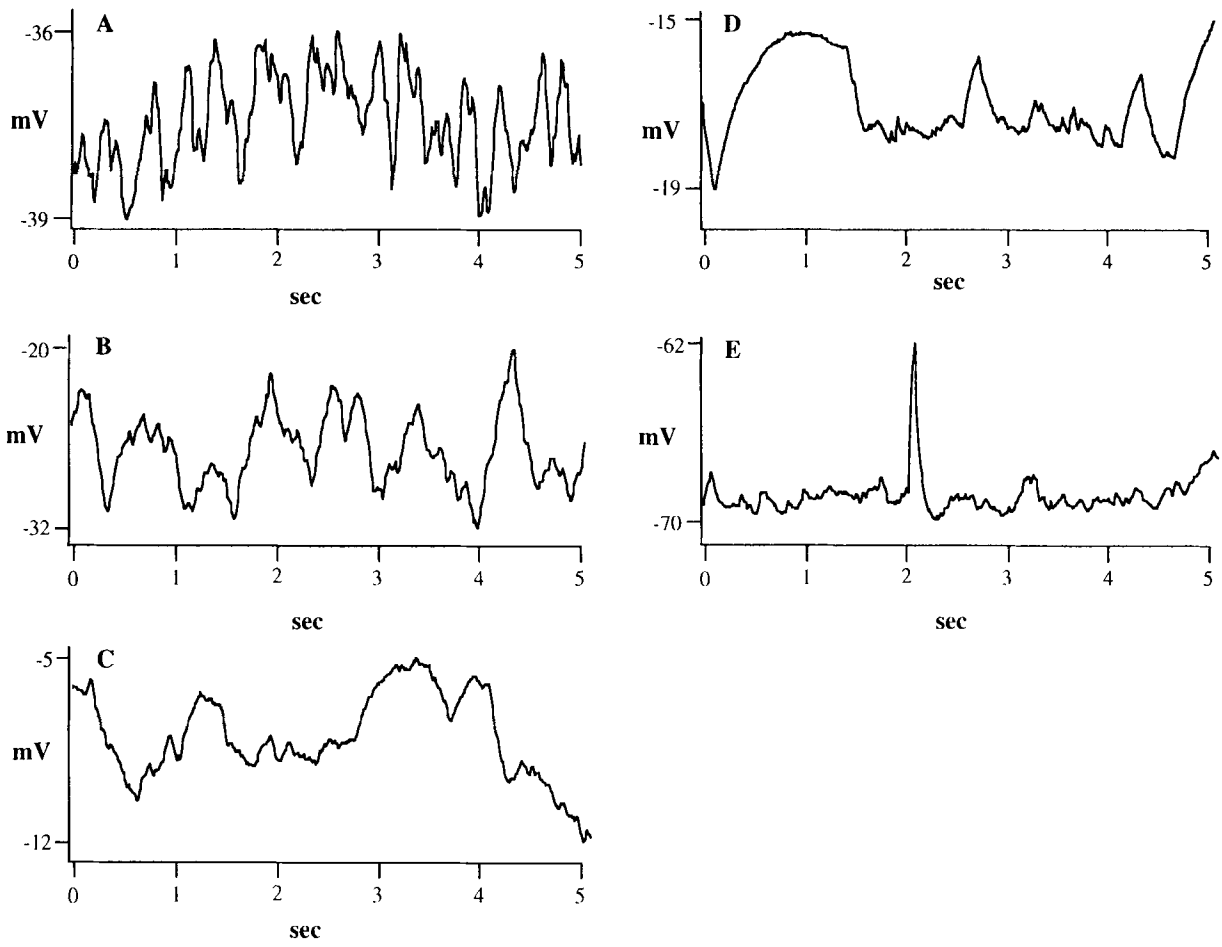

FIGURE 2. Short segment of the membrane potential as a function of time recorded from five different cells illustrating a variety of forms. Each trace consisted of 500 points sampled at 100 points/sec. Therefore, the length of the abscissa is 5 sec for all cells. The maximum and minimum potential in mV between which the membrane potential fluctuated is indicated on the ordinate of each record. The letters A, B, C, D, and E correspond to the murine and human T-cells CL1, CL1, Jurkat, Ka8, and CL1, respectively. The panels in Figs. 2–4 refer to the same cells.

regimes, each of which could be fitted by a straight line, indicated that the time correlations in these cells had fractal properties. The increments of the voltage fluctuations, therefore, are consistent with fGn and have a different value of H in each of the time regimes.

When $H = 0.5$, the changes in the values of a time series are random and, therefore, uncorrelated with each other. When $0 < H < 0.5$, increases in the values of a time series are likely to be followed by decreases and, conversely, decreases are more likely to be followed by increases. Such a time series is called antipersistent. When $0.5 < H < 1.0$, increases in the values of a time series are more likely to be followed by increases, and, conversely, decreases are more likely to be followed by decreases. Such a time series is called persistent (8,22).

The value of H for each of the two regimes was determined from the least squares fit of the logarithm (R/S) *versus* the logarithm (T). The results for each cell are shown in Fig. 3 and Table 1. For these cells, we found that $H = 0.76 \pm 0.05$ (SD) for the short lags (over brief time intervals) and that $H = 0.26 \pm 0.04$ (SD) for the long lags (over long time intervals.) These values of H indicated that there are persistent (positive) correlations over brief time intervals, and there are antipersistent (negative) correlations over long time intervals.

As an additional confirmation of the existence of these correlations, we analyzed the time series generated by randomizing the order of the increments of the membrane potential values. For example, the logarithm (R/S) *versus* logarithm (T) plot for the randomized data from cell E was only one straight line, rather than two regimes, and the slope of the fit determined that $H = 0.54$, indicating that there were no correlations. Therefore, randomizing the order of the data removed the short-term persistent and long-term antipersistent correlations present in the original data. The effect of the spikes in Fig. 2E also was investigated. Spikes were identified in a record and manually replaced with linear interpolated segments. The Hurst coefficient calculated for the records with and without spikes differed by 3%. Therefore, we concluded that infrequent spikes did not noticeably affect the calculation of the Hurst coefficient.

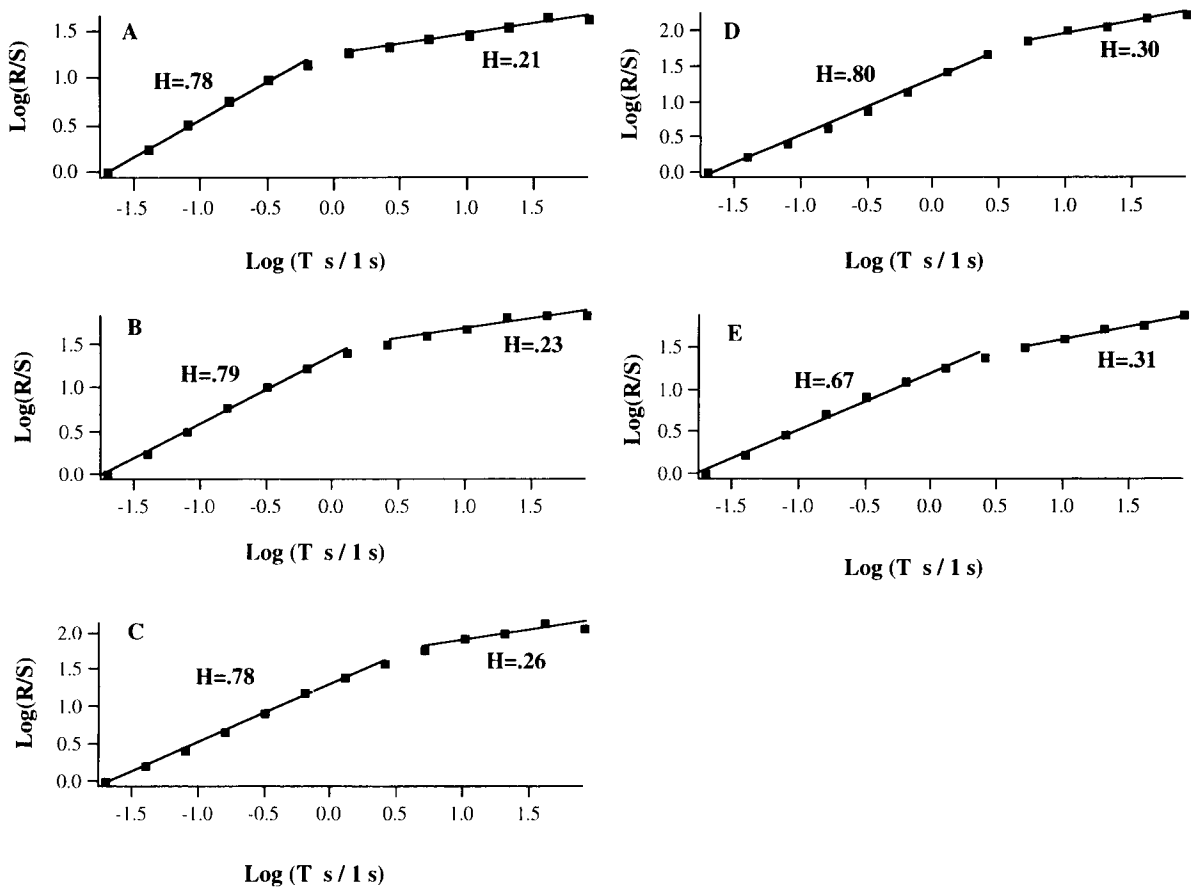

FIGURE 3. Rescaled range analysis of the membrane potential for the five cells. Within each of two regimes Log_{10} (*R/S*) was found to be proportional to Log_{10} (*T s*/1 *s*), where *R* is a measure of the voltage fluctuations within a time window *T* normalized by the standard deviation *S*. The constant of proportionality is called the Hurst exponent *H*. The linearity of these plots indicated that the fluctuations of the membrane potential had a fractal form with a different value of *H* in each regime.

Although the form of the fluctuations of the membrane potential differed markedly in these five cells, the types of time correlations were remarkably similar in each cell. That is, in each cell there were persistent (positive) correlations over brief time intervals and antipersistent (negative) correlations over long time intervals. Moreover, the strength of these correlations in these two regimes, as measured by the Hurst exponent H, was similar for all these cells.

Power Spectrum

The power spectrum, *PS*, of the the differences between successive values of the membrane potential sampled at 0.01 sec is shown in Fig. 4. Moreover, corresponding to what was found from the Hurst rescaled range analysis, there are two distinct regimes for all of the cells. In both regions, the power was approximately proportional to f^{-b}, where where f was frequency. A fractal process, such as fGn, produces such a power law relationship. There-

TABLE 1. *H, b,* and $2H - 1$ for each cell.

	H From the Rescaled Range Analysis $(R/S) \propto T^H$		b From the Power Spectrum Analysis $PS \propto f^{-b}$		$b' = 2H - 1$ Predicted for the Power Spectrum From the *R/S* Analysis	
Cell	Short Lags	Long Lags	Low Frequency	High Frequency	Low Frequency	High Frequency
A	0.78	0.21	−1.36	2.16	−0.58	0.56
B	0.79	0.23	−0.69	1.94	−0.54	0.58
C	0.78	0.26	0.07	1.34	−0.48	0.56
D	0.80	0.30	0.35	1.56	−0.40	0.60
E	0.67	0.31	−0.87	1.50	−0.38	0.34

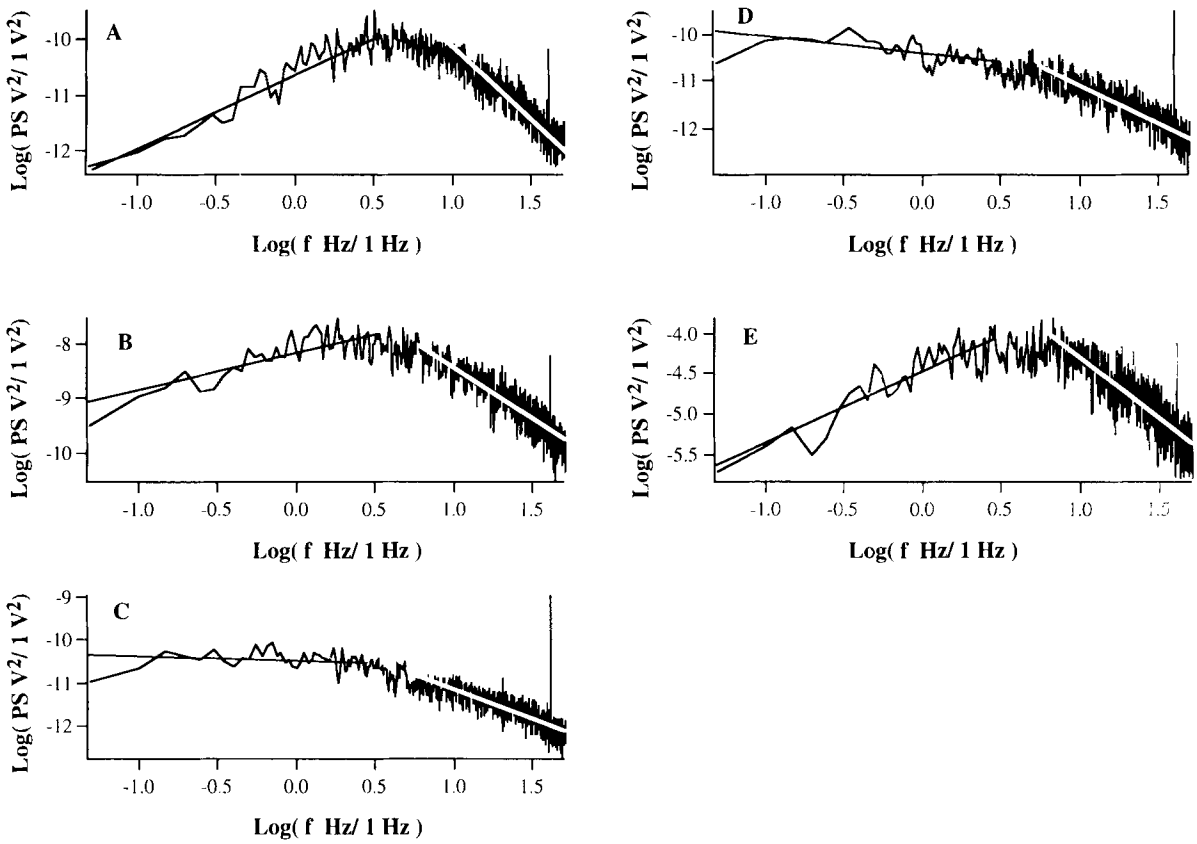

FIGURE 4. Power spectrum, *PS*, of the differences of the membrane potential as a function of frequency *f* for the five cells. Within each of two regimes Log_{10} (*PS* $V^2/1V^2$) was found to be proportional to Log_{10} (*f* Hz/1 Hz). The constant of proportionality was $-b$. The linearity of these plots is consistent with the fact that the fluctuations of the membrane potential have a fractal form with a different value for *b* in each regime.

fore, the existence of regimes that can be fitted by such power law relationships also indicated that the time correlations of the membrane potentials in these cells had fractal properties.

The relationships of the logarithm (*PS*) *versus* the logarithm (*f*) were not exactly linear, as can be seen in the slight curvature of the graphs in Fig. 4. Therefore, the values of *b* depend on the range of frequencies chosen to fit the power law relationship. For consistency, for all cells, we used the values of the power spectrum at frequencies less than 3 Hz and the values of the power spectrum at frequencies greater than 5 Hz to define the low and high frequency regimes for the least squares fit to determine the values of *b*.

For a time series in which the increments are fGn there is a relationship between the exponent *H* determined from the rescaled range analysis of these increments and the exponent *b* determined from the power spectrum of these increments (9). The relationship is $b = 2H - 1$. In Table 1, we list the values of *b* determined directly from the power spectrum and those determined from the values of *H* found from the rescaled range analysis. These values were more similar for some cells than for others and more similar for the low frequency regime than for the high frequency regime. For example, the values found for cell B differed by 0.15, whereas the average difference for the low frequency regime for all five cells was 0.5. For the high frequency regime, the average difference between the values was 1.2.

DISCUSSION

Although a number of studies have used different experimental methods to measure the average electrical potential across the cell membrane of cells, such as T-lymphocytes, very little is known about how this voltage fluctuates in time. Irregular fluctuations have been mentioned as occurring in fibroblasts but have not been analyzed in detail (25).

We used the whole cell patch technique to record the membrane potential across T-lymphocytes as a function of time. As shown in Fig. 1, the fluctuations of the membrane potential appeared to have the form of a fractal process. We tested this hypothesis by using the Hurst rescaled range analysis and power spectrum to analyze the membrane potential as a function of time.

In the rescaled range analysis, the range *R*, normalized

by the standard deviation S, is determined as a function of a time window size T, which was called the lag. We found that, in two different regimes, the logarithm (R/S) was proportional to the logarithm (T). The proportionality constant is called H, the Hurst exponent. This proportionality indicated that the fluctuations in membrane potential had a self-similar, fractal form. We also determined the power spectrum PS of the differences between successive values of the membrane sampled 0.01 sec and found that, in two different regimes, the logarithm (PS) was proportional to the logarithm (f), where f is frequency. This form of the power spectrum also was consistent with a fractal form of the fluctuations in the membrane potential.

The rescaled range analysis showed that $H = 0.76 \pm 0.05$ (SD) for short time lags and that $H = 0.26 \pm 0.04$ (SD) for the long time lags. These values of H indicated that there are persistent (positive) correlations over brief time intervals, whereas there are antipersistent (negative) correlations over long time intervals.

The interpretation would be simpler if there were only one regime in the rescaled range and power spectrum. However, we found that there were two well-defined regimes in the experimental data. Both regimes have the same form, namely linear plots of the logarithm (R/S) *versus* the logarithm (T) and the logarithm (PS) *versus* the logarithm (f), but the slope of each of these relationships was different in each regime. Recently, this same type of behavior also was reported in two other physiological systems. Collins and DeLuca (6) found that the small motions of a person standing quietly had values of $H = 0.83 \pm 0.04$ over brief time intervals and $H = 0.26 \pm 0.06$ over long time intervals. Treffner (32) found that the position in space of the top of a vertical rod being balanced in one hand also had high values of H over brief time intervals and low values of H over long time intervals.

It is quite interesting that the time correlations in the membrane fluctuations have different properties in these two regimes. This may mean that a single, complex, nonlinear process is responsible for the different values of H, or that two different physiological processes are present, one producing positive and the other producing negative correlations.

Each of these two regimes can be characterized by a stochastic process with fractal properties. Such a phenomenological description of the data may provide insight into the nature of the mechanism that produced the data. This stochastic process is consistent with fGn (8,22). The running sum of these increments is fBm (8,22). The rescaled range analysis of the time series of the values of fGn yields a straight line on a plot of the logarithm (R/S) *versus* the logarithm (T) with a slope equal to H. The power spectrum of the time series of the values of fGm yields a straight line on a plot of the logarithm (PS) *versus* the logarithm (f) with slope equal to $-b$. Therefore, these scaling results were consistent with the assumption that the differences between successive values of the membrane potential have the form of fGn, although it does not prove that the membrane potential was produced by this process.

When the time series is fGn, there is a relationship between H determined from the rescaled range analysis and b determined from the power spectrum. This relationship is that $b = 2H - 1$ (9). As shown in Table 1, the accuracy of this relationship varied from one cell to another and was more closely satisfied in the low frequency regime than in the high frequency regime. Schepers *et al.* (30) and Bassingthwaighte and Raymond (3) used test data with known values of H to evaluate the accuracy of different methods in determining H. They found that there were systematic biases between the values of H used to generate the test data and the values of H determined by the rescaled range analysis and other methods. Our own results were consistent with their findings. In addition, they found that these biases were strongly dependent on the length of the time series. Their results indicated that the relationship $b = 2H - 1$ can be in error when H was determined by the rescaled range analysis, and b was determined by the power spectra. Moreover, they found that these errors were larger for smaller values of H. Therefore, the discrepancies in satisfying this relationship that we found could be partly caused by the errors in determining H and b. They also may indicate that the fluctuations in the membrane voltage do not have exactly the form of fGn.

Although the fluctuations of the membrane potential have very different forms in different cells, they all have the same common feature of a fractal form with persistent (positive) correlations over brief time intervals and antipersistent (negative) correlations over long time intervals. Therefore, the fractal nature of these fluctuations and their time correlations may provide a way to characterize the membrane potential and to measure the changes that occur when T-lymphocytes were activated.

These membrane fluctuations have fractal properties, which means that the methods used for the analysis of the temporal characteristics of the membrane voltage must take these properties into account. For example, the moments of fractal time series, such as the mean and standard deviation are not defined. That is, these moments depend on the amount of data analyzed and do not reach finite limiting values as the amount of data is increased. Therefore, any method of analysis that assumes that the membrane potential is Gaussian or asymptotically Gaussian is not sufficiently general to adequately analyze the properties of the membrane potentials of these cells.

Models of the membrane potential used in the past often were based on such Gaussian or asymptotically Gaussian random variables. This has led to the assumption, stated explicitly or assumed implicitly, that elements

in a time series representing fluctuating experimentally determined quantities are not correlated if they are sufficiently far apart in time.

However, if the time series is produced by a persistent or antipersistent process, then the elements of the time series are correlated no matter how far apart in time they occurred. For such a process, the correlation (normalized by the variance) between a point at time $-t$ in the past and a point $+t$ in the future depends only on the value of H and not on the magnitude of t (eq. 9.16 in Reference 8). Such correlations cannot be represented by simple linear kinetic models that have a Lorentzian power spectrum (1,7). Such linear models display fractal behavior only when they incorporate a very large number of individual components. The fractal form of the correlations is then represented by relationships between the large number of parameters of the linear components. For example, this is the case when the time constants of the many Markov components form a geometric progression (13,23).

The membrane potential depends on the opening and closing of ion channels in the cell membrane. Independent of our work presented herein, two other groups have predicted that fractal fluctuations in the membrane voltage may arise from either nonlinear interactions between different ion channels (17,18) or the non-Markovian kinetics of individual ion channels (17,18,28).

REFERENCES

1. Ball, F. G., G. F. Yeo, R. K. Milne, R. O. Edeson, B. W. Madsen, and M. S. P. Sansom. Single ion channel models incorporating aggregation and time interval omission. *Biophys. J.* 64:357–374, 1993.
2. Bassingwaighte, J. B., L. S. Liebovitch, and B. J. West. *Fractal Physiology*. New York: Oxford University Press, 1994, 364 pp.
3. Bassingwaighte, J. B., and G. M. Raymond. Evaluating rescaled range analysis for time series. *Ann. J. Biomed. Eng.* 22:432–444, 1994.
4. Brigham, E. O. *The Fast Fourier Transform and Its Applications*. Englewood Cliffs, NJ: Prentice Hall, 1988, 448 pp.
5. Cahalan, M. D., K. G. Chandy, T. E. DeCoursey, and S. Gupta. A voltage-gated potassium channel in human T-lymphocytes. *J. Physiol.* 358:197–237, 1985.
6. Collins, J. J. and C. J. DeLuca. Random walking during quiet standing. *Phys. Rev. Lett.* 73:764–767, 1994.
7. DeFelice, L. J. *Introduction to Membrane Noise*. New York: Plenum Press, 1981, 500 pp.
8. Feder, J. *Fractals*. New York: Plenum Press, 1988, 283 pp.
9. Flandrin, P. On the spectrum of fractional Brownian motions. *IEEE Trans. Infor. Theor.* 35:197–199, 1989.
10. Gallin, E. K. Ion channels in leukocytes. *Physiol. Rev.* 71: 775–811, 1991.
11. Grinstein, S., and S. J. Dixon. Ion transport, membrane potential, and cytoplasmic pH in lymphocytes: changes during activation. *Physiol Rev.* 69:417–481, 1989.
12. Hurst, H. E., R. P. Black, and Y. M. Simaika. *Long-Term Storage, An Experimental Study*. London: Constable, 1965, 145 pp.
13. Liebovitch, L. S. Analysis of fractal ion channel gating kinetics: kinetic rates, energy levels, and activation energies. *Math. Biosci.* 93:97–115, 1989a.
14. Liebovitch, L. S. Introduction to the properties and analysis of fractal objects, processes, and data. In: *Advanced Methods of Physiological System Modeling*, edited by V. Z. Marmarelis. New York: Plenum Press, 1989b, pp. 225–239.
15. Liebovitch, L. S., and T. I. Toth. Using fractals to understand the opening and closing of ion channels. *Ann. J. Biomed. Eng.* 18:177–194, 1990.
16. Liebovitch, L. S. Introduction to fractals in biology. *Trans. Tut. IEEE Engr. Med. Biol. Soc. Meet:*, Paris, France, 1992.
17. Lowen, S. B., and M. C. Teich. Fractal auditory nerve firing patterns may derive from fractal switching in sensory hair-cell ion channels. In: *Noise in Physical Systems Systems and 1/f Fluctuations*, edited by P. H. Handel and A. L. Chung. New York: American Institute of Physics, AIP Conference Proceedings, 285, 1993a, pp. 781–784.
18. Lowen, S. B., and M. C. Teich. Fractal renewal processes. *IEEE Trans. Infor. Theor.* 39:1669–1671, 1993b.
19. Lundahl, T., W. J. Ohley, S. M. Kay, and R. Siffert. Fractional Brownian motion: a maximum likelihood estimator and its application to image texture. *IEEE Trans. Med. Imaging* 5:152–161, 1986.
20. Maltsev, V. A. Oscillating and triggering properties of T cell membrane potential. *Immun. Lett.* 26:277–282, 1990.
21. Maltsev, V. A. A negative resistance region underlies the triggering property of membrane potential in human T-lymphocytes. *Cell Signaling* 4:697–707, 1992.
22. Mandelbrot, B. B. *The Fractal Geometry of nature*. Salt Lake City, UT: W. H. Freeman and Company, 1982, pp. 247–255, 386–387, and 396–398.
23. Millhauser, G. L., E. E. Salpeter, and R. E. Oswald. Rate amplitude correlation from single channel records. *Biophys. J.* 54:1165–1168, 1988.
24. Niemtzow, R. C. *Transmembrane Potentials and Characteristics of Immune and Tumor Cells*. Boca Raton, FL: CRC Press Inc, 1985, 159 pp.
25. Oiki, S., and Y. Okada. Factors responsible for oscillations of membrane potential recorded with tight-seal-patch electrodes in mouse fibroblasts *J. Membr. Biol.* 105:23–32, 1988.
26. Peters, E. E. *Chaos and Order in the Capital Markets*. New York: John Wiley & Sons, 1991, 240 pp.
27. Press, W. H., B. P. Flannery, S. A. Teukolsky, and W. T. Vetterling. *Numerical Recipes*, (second edition). New York: Cambridge University Press, 1992, 994 pp.
28. Roncaglia, R., R. Mannell, and P. Grigonlini. Fractal properties of ionic channels and diffusion, *Math. Biosci.* 123:77–101, 1994.
29. Sakmann, B., E. Neher, ed. *Single-Channel Recording*. New York: Plenum Press, 1983, 501 pp.
30. Schepers, H. E., J. H. G. M. van Beek, and J. B. Bassingthwaighte. Four methods to estimate the fractal dimension from self-affine signals. *IEEE Eng. Med. Biol. Mag.* June:57–71, 1992.
31. Yeandle, S., and W. A. Gottschalk. *Pulse and Trapezoidal Voltage Clamps Applied to Jurkat Cells, a T-lymphocyte Cell Line*. Bethesda, MD: Naval Medical Research Institute Report, 1993, 14 pp.
32. Treffner, P. J. and J.A.S. Kelso. Functional stabilization of unstable fixed-points. In: Studies in Perception and Action: Proceedings of the International Conference on Perception and Action, edited by B. Bardy, R. Bootsma and Y. Guiard. Mahwah, NJ: Erlbaum, 1995, pp. 83–86.